Meteoritics & Planetary Science 37, 1361–1376 (2002)
Available online at http://www.uark.edu/meteor

Size-frequency distributions of chondrules and chondrule fragments in LL3 chondrites: Implications for parent-body fragmentation of chondrules

VICTORIA E. NELSON AND ALAN E. RUBIN*

Institute of Geophysics and Planetary Physics, University of California, Los Angeles, California 90095-1567, USA
*Correspondence author's e-mail address: aerubin@ucla.edu

(Received 2001 March 12; accepted in revised form 2002 June 21)

Abstract–We measured the sizes and textural types of 719 intact chondrules and 1322 chondrule fragments in thin sections of Semarkona (LL3.0), Bishunpur (LL3.1), Krymka (LL3.1), Piancaldoli (LL3.4) and Lewis Cliff 88175 (LL3.8). The mean apparent diameter of chondrules in these LL3 chondrites is 0.80 ϕ units or 570 μm, much smaller than the previous rough estimate of ~900 μm. Chondrule fragments in the five LL3 chondrites have a mean apparent cross-section of 1.60 ϕ units or 330 μm. The smallest fragments are isolated olivine and pyroxene grains; these are probably phenocrysts liberated from disrupted porphyritic chondrules. All five LL3 chondrites have fragment/chondrule number ratios exceeding unity, suggesting that substantial numbers of the chondrules in these rocks were shattered. Most fragmentation probably occurred on the parent asteroid. Porphyritic chondrules (porphyritic olivine + porphyritic pyroxene + porphyritic olivine–pyroxene) are more readily broken than droplet chondrules (barred olivine + radial pyroxene + cryptocrystalline). The porphyritic fragment/chondrule number ratio (2.0) appreciably exceeds that of droplet-textured objects (0.9). Intact droplet chondrules have a larger mean size than intact porphyritic chondrules, implying that large porphyritic chondrules are fragmented preferentially. This is consistent with the relatively low percentage of porphyritic chondrules within the set of the largest chondrules (57%) compared to that within the set of the smallest chondrules (81%). Differences in mean size among chondrule textural types may be due mainly to parent-body chondrule-fragmentation events and not to chondrule-formation processes in the solar nebula.

INTRODUCTION

The principal components of type-3 ordinary chondrites (OC) are chondrules, chondrule fragments, isolated mafic silicate grains, fine-grained silicate matrix material, metallic Fe-Ni and sulfide. The fundamental characteristics of these components are size, shape, texture, mineralogy and composition. Many studies have focused on chondrule compositions, but relatively few on chondrule size-frequency distributions. Some studies of chondrule sizes do not distinguish chondrule textural types (*e.g.*, Dodd, 1976; King and King, 1978, 1979; Martin and Mills, 1976, 1978). Other studies compare chondrule size and textural type, but ignore the size-frequency distributions of chondrule fragments (*e.g.*, Gooding and Keil, 1981; Nagahara, 1981; Rubin and Keil, 1984).

The present study is a determination of the size-frequency distributions of different textural types of chondrules and chondrule fragments >88 μm in diameter in thin sections of five LL3 chondrites. In addition to determining data relating to chondrule size, the study has the ancillary aims of finding out which textural types of chondrules are more readily broken, and ascertaining whether chondrule fragmentation occurred mainly in the solar nebula or on a parent asteroid.

ANALYTICAL PROCEDURES

We examined thin sections of five LL3 chondrites (Table 1) microscopically in transmitted and reflected light. We enlarged transmitted-light photomicrographs of the thin sections; typical enlargements were 0.5–1 m across. Each chondrule, chondrule fragment and isolated silicate grain >88 μm in maximum dimension was located, numbered and measured on the photographs. About 10 chondrules in each thin section were measured in transmitted light on the petrographic microscope using a calibrated reticle. Chondrule sizes on the photographs were normalized to those obtained microscopically. The sizes of all chondrules and fragments that appeared too dark on the photographs for easy measurement were determined microscopically. For every object, size was determined by averaging the measurement of the maximum dimension (**a**) and the maximum dimension (**b**) that is perpendicular to **a**. This measurement is called apparent diameter for chondrules and apparent cross-section for chondrule fragments. Axial ratios

Prelude preprint MS#4523

© Meteoritical Society, 2002. Printed in USA.

TABLE 1. LL3 chondrites examined in the present study.

Chondrite	Subtype	Shock stage	Thin section	#chd	#frag
Bishunpur	LL3.1	S2	B-80339	86	310
Krymka	LL3.1	S3	USNM 1729-3	91	261
LEW 88175	LL3.8	S1	LEW 88175,11	75	117
Piancaldoli	LL3.4	S1	USNM 5649	87	152
Semarkona	LL3.0	S2	USNM 1805-3	67	78
Semarkona	LL3.0	S2	USNM 1805-5	94	38
Semarkona	LL3.0	S2	UNM 312	66	159
Semarkona	LL3.0	S2	LC 229	19	8
Semarkona	LL3.0	S2	AMNH 4128-2	77	88
Semarkona	LL3.0	S2	AMNH 4128-4	57	111

Abbreviations: #chd = number of intact chondrules; #frag = number of chondrule fragments; LEW = Lewis Cliff; AMNH = American Museum of Natural History; B = Natural History Museum (London); LC = UCLA Leonard Collection; UNM = University of New Mexico; USNM = Smithsonian Institution.

are defined as **b/a**. Identifications of the textural types of chondrules, chondrule fragments and isolated mineral grains were made microscopically.

Standard abbreviations are used for chondrule and chondrule-fragment textural types: POP = porphyritic olivine–pyroxene, PP = porphyritic pyroxene, PO = porphyritic olivine, BO = barred olivine, RP = radial pyroxene, C = cryptocrystalline, and GOP = granular olivine-pyroxene. Because it was too difficult to distinguish reliably low-FeO type-I from high-FeO type-II porphyritic chondrules (*e.g.*, Figs. 1–3 of Scott and Taylor, 1983) in the petrographic microscope, these types were lumped together.

Chondrules were deemed intact if they exhibited ≥270° of arc. Objects with less than this amount of curvature (including objects with highly irregular surfaces) were classified as fragments. Monomineralic isolated mafic silicate grains were listed separately irrespective of their shapes and were classified as fragments. Each pair or set of compound chondrules was measured and counted as a single object; the textural type was considered to be that of the largest component in the compound object.

Chondrule apparent diameters and chondrule-fragment apparent cross-sections are listed in Table 2 in ϕ units which are defined by the relationship $\phi = -\log_2 d$, where d is the average apparent diameter of the chondrule (or the average apparent cross-section of the fragment) in millimeters. Because it was difficult to identify and measure every chondrule fragment smaller than 88 μm (3.5 ϕ units), only chondrules, chondrule fragments and isolated mafic silicate grains larger than this limit were measured.

The major disadvantage of this approach (as in all thin-section size studies) is that true chondrule sizes are underestimated; only apparent sizes are measured. Hughes (1978) reported that the mean and median apparent diameters of chondrules measured in thin section are $\sqrt{(2/3)}$ and $\sqrt{(3/4)}$, respectively, of the actual mean and median diameters (D). Eisenhour (1996) noted that the mean apparent diameter is $(\pi/4)D$ instead of $\{\sqrt{(2/3)}\}D$. These corrections to apparent chondrule sizes cannot be applied to chondrule fragments because of the irregular shapes of many of these objects. All of the data presented here are uncorrected.

Grady (2000) listed a total of 71 LL3 chondrites, of which nine are falls. One of these falls is Chainpur, which Wasson and Wang (1991) listed as an L/LL3 chondrite because its kamacite Co contents are outside the nominal LL-chondrite range (Rubin, 1990). Thus, although the five LL3 chondrites studied here (four falls, one find) represent only 7% of known LL3 chondrites, they include 50% of well-classified LL3 falls. The significant degree of weathering of many LL3 finds renders such rocks unsuitable for detailed studies of small chondrule fragments.

RESULTS

Chondrules

Chondrule Sizes in LL3 Chondrites–Figure 1a shows that the 719 LL chondrules have a log-normal size-frequency distribution with a peak at 0.5–1.0 ϕ units (500–707 μm) and an average apparent diameter of 0.80 ϕ units (570 μm) (Table 2). The mean chondrule size was determined in ϕ units and then converted into micrometers. All of the chondrules were lumped together for the determination of the average diameter. Because a plurality of chondrules is from Semarkona (Table 1), the mean diameter is biased toward that of Semarkona chondrules. The standard deviation of the sampling distribution ($\sigma/\sqrt{n}$) is 22 μm where σ is the sample standard deviation and n is the total number of chondrules.

The newly determined average LL chondrule size (570 μm) is in good agreement with the mean value we obtained from

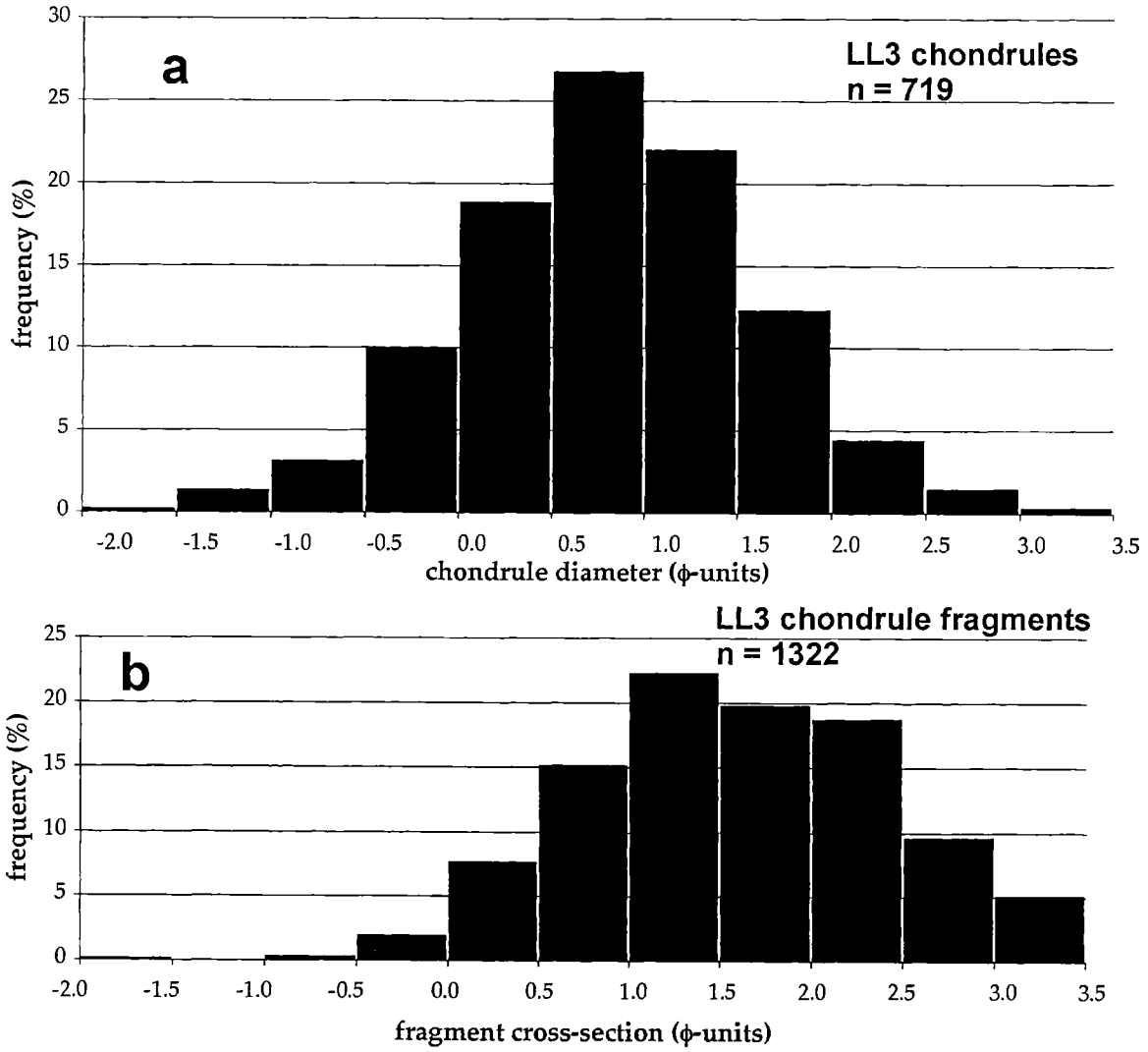

FIG. 1. Size-frequency distributions of chondrules and chondrule fragments measured in thin section in five LL3 chondrites. (a) The 719 chondrules have a mean apparent diameter of 0.80 ϕ units (570 μm). (b) The 1322 chondrule fragments have a mean apparent cross-section of 1.60 ϕ units (330 μm). The fragments are significantly smaller than the intact chondrules.

Fig. 1 of Benoit *et al.* (1999) (*i.e.*, 0.91 ϕ units (530 μm)). However, these values are appreciably smaller than the former rough estimate of 900 μm (Grossman *et al.*, 1988) based on previous, much more limited studies (King and King, 1979; Gooding, 1979; Rubin and Keil, 1984). (King and King (1979) measured apparent diameters of 45 chondrules from a single LL chondrite (Parnallee, LL3.7). Gooding (1979) measured the true sizes of a total of 46 chondrules separated from three LL chondrites (Chainpur, LL3.4; Semarkona, LL3.0; Ngawi, LL3.6), but his separation technique excluded all LL3 chondrules with diameters smaller than 510 μm. Only four LL3 chondrules in his set are <700 μm in diameter. Rubin and Keil (1984) made thin section measurements of 374 chondrules in Inman (L/LL3.4), but included only BO, RP and C textural types.)

Within two standard deviations of the sampling distribution, four of the five LL3 chondrites in the present study have the same mean chondrule sizes: LL3.0 Semarkona (0.72 ϕ units; 610 μm) (Fig. 2a); LL3.4 Piancaldoli (0.74 ϕ units; 600 μm); LL3.1 Bishunpur (0.76 ϕ units; 590 μm); LL3.1 Krymka (0.94 ϕ units; 520 μm); and LL3.8 Lewis Cliff (LEW) 88175 (1.19 ϕ units; 440 μm) (Table 2). Although chondrules in LEW 88175 are smaller than those in Semarkona, Piancaldoli and Bishunpur, they are not significantly smaller than those in Krymka. The Krymka chondrule size-frequency distribution (Fig. 2b) is asymmetric, exhibiting a paucity of large chondrules.

Table 3 shows that the range in mean chondrule sizes among the six thin sections of Semarkona is 200 μm: USNM 1805-3 (0.56 ϕ units; 740 μm); USNM 1805-5 (0.93 ϕ units; 620 μm); UNM 312 (0.76 ϕ units; 700 μm); LC 229 (0.54 ϕ units; 790 μm);

TABLE 2. Apparent sizes and axial ratios of chondrules and chondrule fragments in LL3 chondrites.

Chondrite	No. of chds	No. of frags	Chondrule size range	Fragment size range	Chd mean diameter	St. dev.	Frag mean cross-section	St. dev.	Chd mean axial ratio (b/a)	St. dev.	Frag mean axial ratio (b/a)	St. dev.
Semarkona	380	482	3.22 to −1.30 ϕ (110 to 2470 μm)	3.50 to −1.63 ϕ (89 to 3090 μm)	0.72 ϕ (610 μm)	0.80 ϕ	1.38 ϕ (380 μm)	0.85 ϕ	0.81	0.13	0.67	0.17
Bishunpur	86	310	2.39 to −1.24 ϕ (190 to 2360 μm)	3.44 to −0.75 ϕ (92 to 1680 μm)	0.76 ϕ (590 μm)	0.67 ϕ	1.95 ϕ (260 μm)	0.80 ϕ	0.75	0.15	0.66	0.15
Krymka	91	261	3.05 to −1.64 ϕ (120 to 3110 μm)	3.44 to −0.48 ϕ (92 to 1400 μm)	0.94 ϕ (520 μm)	0.80 ϕ	1.80 ϕ (290 μm)	0.78 ϕ	0.80	0.12	0.63	0.16
Piancaldoli	87	152	2.54 to −0.71 ϕ (170 to 1630 μm)	3.01 to −0.30 ϕ (120 to 1230 μm)	0.74 ϕ (600 μm)	0.60 ϕ	1.26 ϕ (420 μm)	0.70 ϕ	0.82	0.12	0.67	0.16
LEW 88175	75	117	3.00 to −0.67 ϕ (130 to 1590 μm)	3.39 to −0.08 ϕ (95 to 1060 μm)	1.19 ϕ (440 μm)	0.76 ϕ	1.53 ϕ (350 μm)	0.66 ϕ	0.85	0.12	0.70	0.15
All objects	719	1322	3.22 to −1.64 ϕ (110 to 3110 μm)	3.50 to −1.63 ϕ (89 to 3090 μm)	0.80 ϕ (570 μm)	0.77 ϕ	1.60 ϕ (330 μm)	0.84 ϕ	0.82	0.12	0.66	0.16

Abbreviations: Chd = chondrules; frags = chondrule fragments; St. dev. = standard deviation; LEW = Lewis Cliff.

TABLE 3. Apparent sizes and axial ratios of chondrules and chondrule fragments in different thin sections of Semarkona.

Section	No. of chds	No. of frags	Chondrule size range	Fragment size range	Chd mean diameter	St. dev.	Frag mean cross-section	St. dev.	Chd mean axial ratio (b/a)	St. dev.	Frag mean axial ratio (b/a)	St. dev.
USNM 1805-3	67	78	2.02 to −1.04 ϕ (250 to 2060 μm)	2.56 to −1.63 ϕ (170 to 3090 μm)	0.56 ϕ (740 μm)	0.62 ϕ	0.88 ϕ (620 μm)	0.72 ϕ	0.82	0.12	0.73	0.18
USNM 1805-5	94	38	2.83 to −0.99 ϕ (140 to 1990 μm)	3.50 to 0.30 ϕ (90 to 810 μm)	0.93 ϕ (620 μm)	0.84 ϕ	1.63 ϕ (380 μm)	0.90 ϕ	0.76	0.14	0.64	0.13
UNM 312	66	159	3.22 to −1.02 ϕ (110 to 2030 μm)	3.45 to −0.18 ϕ (90 to 1140 μm)	0.76 ϕ (700 μm)	0.85 ϕ	1.65 ϕ (380 μm)	0.85 ϕ	0.83	0.12	0.63	0.17
LC 229	19	8	1.83 to −0.41 ϕ (280 to 1330 μm)	3.24 to 0.50 ϕ (110 to 710 μm)	0.54 ϕ (790 μm)	0.79 ϕ	1.35 ϕ (450 μm)	0.93 ϕ	0.84	0.14	0.64	0.21
AMNH 4128-2	77	88	1.97 to −1.30 ϕ (260 to 2470 μm)	3.07 to −0.88 ϕ (120 to 1840 μm)	0.48 ϕ (820 μm)	0.74 ϕ	0.98 ϕ (560 μm)	0.60 ϕ	0.84	0.10	0.68	0.14
AMNH 4128-4	57	111	2.70 to −1.18 ϕ (150 to 2260 μm)	3.38 to −0.42 ϕ (100 to 1390 μm)	0.88 ϕ (630 μm)	0.80 ϕ	1.53 ϕ (410 μm)	0.83 ϕ	0.81	0.14	0.68	0.17

Abbreviations: Chd = chondrules; frags = chondrule fragments; St. dev. = standard deviation.

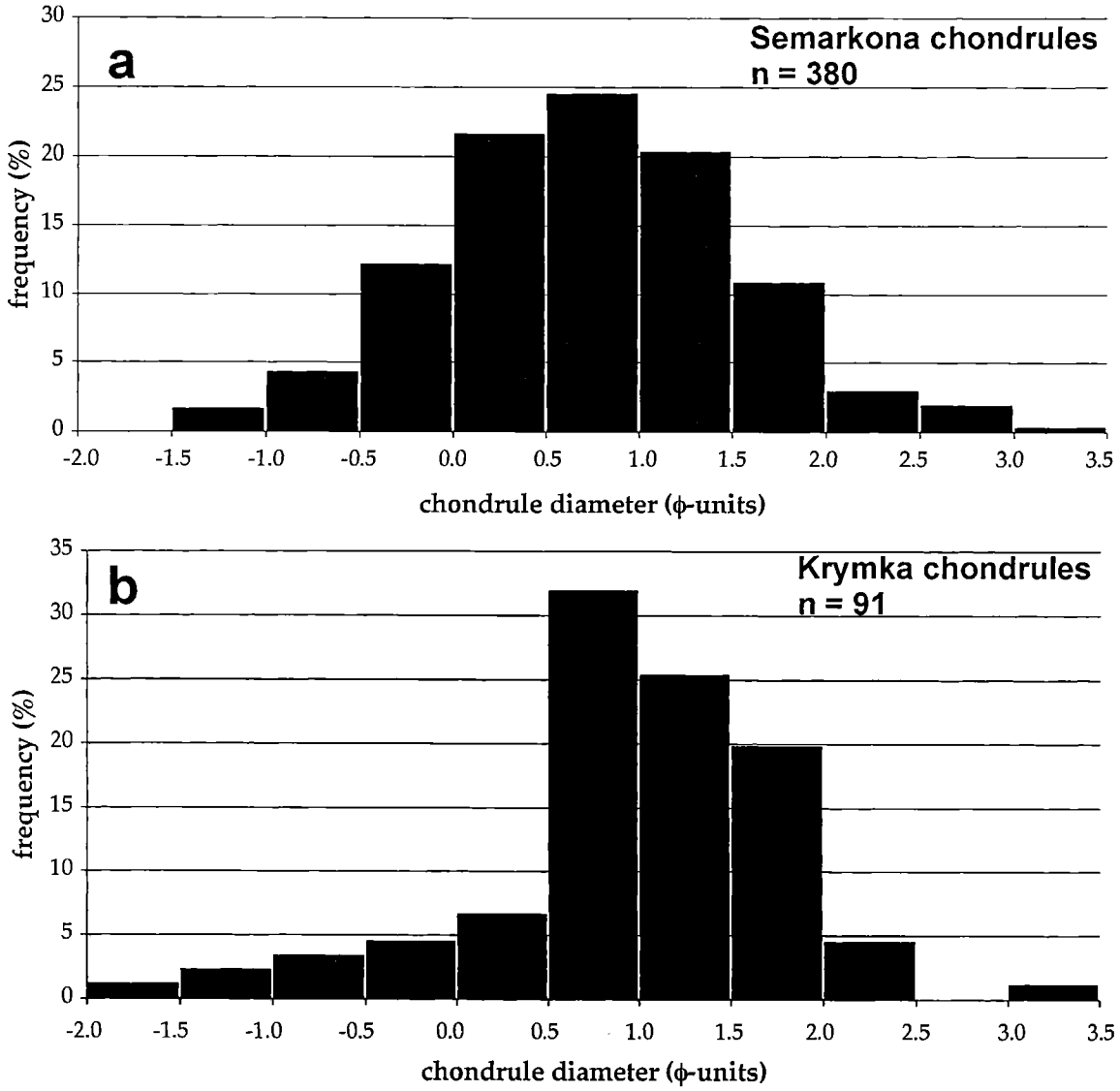

FIG. 2. Size-frequency distributions of chondrules in two LL3 chondrites. (a) The 380 chondrules measured in six thin sections of LL3.0 Semarkona. The mean apparent diameter of the chondrules is 0.72 ϕ units (610 μm). (b) The 91 chondrules measured in thin section in LL3.1 Krymka. The mean apparent diameter of the chondrules is 0.94 ϕ units (520 μm). Chondrules in Krymka have a skewed distribution; there is a paucity of large chondrules.

AMNH 4128-2 (0.48 ϕ units; 820 μm); and AMNH 4128-4 (0.88 ϕ units; 630 μm). This range is greater than that of the mean chondrule sizes in the five different LL3 chondrites studied here (170 μm).

The relatively large mean size of the 86 Bishunpur chondrules (Fig. 3a) is due mainly to the occurrence of 11 large PO chondrules (0.0–0.5 ϕ units) (Fig. 3b) that skew the size-frequency distribution of the entire set of Bishunpur chondrules toward larger sizes.

Proportions of Different Chondrule Textural Types–The number percentages of different chondrule textural types in the five LL3 chondrites are: 47% POP, 21% PP, 16% PO, 6% BO, 3% RP, 4% C and 3% GOP. These proportions are somewhat different than those listed for OC in Rubin (1989a) based on tabulations of previous, more-limited studies (48% POP, 10% PP, 23% PO, 4% BO, 7% RP, 5% C and 3% GOP). In the present study, there are substantially more PP, fewer PO and appreciably fewer RP chondrules.

The proportions of different chondrule textural types vary from one meteorite to another and even between different regions of the same meteorite. Six different thin sections of LL3.0 Semarkona were analyzed; of the five large sections (each of which had 57–94 intact chondrules), the proportion of all chondrules that have PP textures varies from 14% to 41%. Among the different LL3 chondrites, the proportion of PP chondrules varies from 5% in Bishunpur to 25% in LEW 88175.

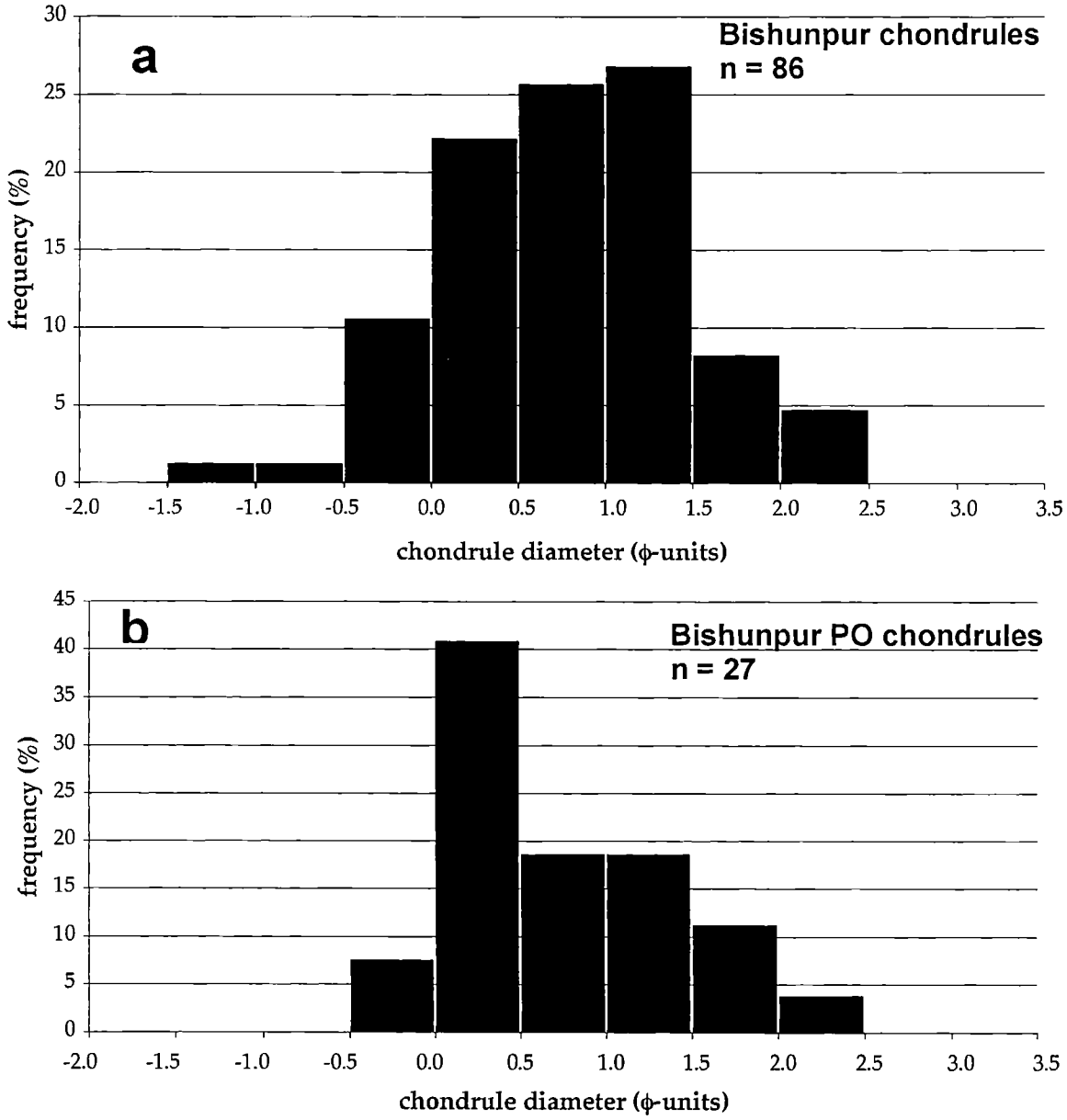

FIG. 3. Chondrule size-frequency distributions in Bishunpur. (a) The 86 Bishunpur chondrules are skewed toward large sizes. They have an anomalously high peak at 0.0–0.5 ϕ units. This peak is due mainly to the large number of PO chondrules in this size range. (b) The 27 PO chondrules in Bishunpur showing a very high peak at 0.0–0.5 ϕ units. This peak may be due to unrepresentative sampling.

These differences probably reflect unrepresentative (*i.e.*, insufficient) sampling and, hence, are not statistically meaningful.

The proportions of different chondrule textural types differ at different size intervals (Table 4) (*i.e.*, different textural types have different mean diameters). Among the 43 smallest chondrules (those $\geq$2.0 ϕ units or $\leq$177 μm in apparent diameter), 53% are POP, 23% are PP, 5% are PO, 7% are C, 7% are BO, 5% are GOP and 0% are RP. Among the 32 largest chondrules (those less than or equal to –0.5 ϕ units or $\geq$1414 μm in apparent diameter), 25% are POP, 13% are PP, 19% are PO, 9% are C, 22% are BO, 0% are GOP and 12% are RP. Thus, porphyritic chondrules constitute 81% of small chondrules but only 57% of large chondrules (*i.e.*, as chondrule size increases the proportion of porphyritic chondrules decreases). The combined set of nonporphyritic (RP, C, GOP) and BO chondrules constitutes 19% of small chondrules and 43% of large chondrules. Because many nonporphyritic and BO chondrules in ordinary chondrites are FeO-rich (*e.g.*, Tables 1 and 3 of Grossman and Wasson, 1982; Table 1 of Grossman and Wasson, 1985), we infer that the proportion of FeO-rich chondrules in LL3 chondrites increases with increasing chondrule size.

TABLE 4. Proportions of chondrule types in different apparent size intervals for LL3 chondrites.

Size interval		Percentage of all chondrules							Total no. of chds.
Diameter (μm)	Diameter (ϕ units)	RP	C	GOP	BO	PO	PP	POP	
2828 to 4000	−2.0 to −1.5	–	100	–	–	–	–	–	1
2000 to 2828	−1.5 to −1.0	11.1	–	–	44.4	11.1	22.2	11.1	9
1414 to 2000	−1.0 to −0.5	13.6	9.1	–	13.6	22.7	9.1	31.8	22
1000 to 1414	−0.5 to 0.0	9.9	4.2	1.4	9.9	15.5	14.1	45.1	71
707 to 1000	0.0 to 0.5	0.7	3.7	2.2	7.4	25.9	19.3	40.8	135
500 to 707	0.5 to 1.0	1.6	1.6	4.2	3.1	15.6	21.9	52.4	192
354 to 500	1.0 to 1.5	0.6	5.1	2.5	2.5	12.0	23.4	53.8	158
250 to 354	1.5 to 2.0	2.3	6.8	5.7	3.4	13.6	25.0	43.2	88
177 to 250	2.0 to 2.5	–	6.5	–	6.5	3.2	29.0	54.8	31
125 to 177	2.5 to 3.0	–	10.0	20.0	–	10.0	10.0	50.0	10
88 to 25	3.0 to 3.5	–	–	–	50.0	–	–	50.0	2

Abbreviations: chds. = chondrules; RP = radial pyroxene; C = cryptocrystalline; GOP = granular olivine-pyroxene; BO = barred olivine; PO = porphyritic olivine; PP = porphyritic pyroxene; POP = porphyritic olivine–pyroxene.

TABLE 5. Apparent sizes and axial ratios of different chondrule types in LL3 chondrites.

Chondrule type	Number of chds.	Size range	Mean diameter	St. dev. (ϕ)	Mean axial ratio (b/a)	St. dev.
RP	18	1.88 to −1.02 ϕ (270 to 2030 μm)	0.16 ϕ (900 μm)	0.87	0.85	0.12
C	31	2.70 to −1.64 ϕ (150 to 3110 μm)	0.83 ϕ (560 μm)	0.88	0.84	0.14
GOP	23	2.83 to −0.07 ϕ (140 to 1050 μm)	1.13 ϕ (460 μm)	0.69	0.74	0.13
BO	40	3.05 to −1.32 ϕ (120 to 2500 μm)	0.41 ϕ (750 μm)	1.02	0.81	0.12
PO	115	2.83 to −1.04 ϕ (140 to 2060 μm)	0.60 ϕ (660 μm)	0.68	0.82	0.13
PP	151	2.54 to −1.24 ϕ (170 to 2360 μm)	0.91 ϕ (530 μm)	0.71	0.80	0.12
POP	341	3.22 to −1.17 ϕ (110 to 2250 μm)	0.88 ϕ (540 μm)	0.72	0.82	0.12
All chds	719	3.22 to −1.64 ϕ (110 to 3110 μm)	0.80 ϕ (570 μm)	0.77	0.82	0.12

Abbreviations: chds. = chondrules; St. dev. = standard deviation; RP = radial pyroxene; C = cryptocrystalline; GOP = granular olivine-pyroxene; BO = barred olivine; PO = porphyritic olivine; PP = porphyritic pyroxene; POP = porphyritic olivine–pyroxene.

Size-frequency Distributions of Different Chondrule Textural Types–Chondrules in LL3 chondrites can be placed in order of decreasing mean apparent diameter (Table 5): RP (0.16 ϕ, 900 μm), BO (0.41 ϕ, 750 μm), PO (0.60 ϕ, 660 μm), C (0.83 ϕ, 560 μm), POP (0.88 ϕ, 540 μm), PP (0.91 ϕ, 530 μm), GOP (1.13 ϕ, 460 μm). A series of Kolmogorov–Smirnov two-sample one-tailed statistical tests (Till, 1974) using interval widths of 0.5 ϕ units was performed to test the hypothesis that one textural type of chondrule is significantly larger than another. This is a non-parametric test commonly used to compare two population distributions of unknown form; normality is not required.

As shown in Table 6, PO chondrules are significantly larger than PP and POP chondrules. BO chondrules are larger than PO chondrules, the entire set of porphyritic chondrules (PO, PP, POP), and the entire set of nonporphyritic chondrules (RP, C, GOP).

The set of 72 nonporphyritic chondrules has a larger size than that of the 607 porphyritic chondrules. This overall size difference is due entirely to the large sizes of the 18 RP chondrules in the set which are significantly larger than PO

TABLE 6. Statistical significance of differences among textural types of intact chondrules.

Chondrule sets	χ^{2*}	Confidence level
PP ≈ POP	0.46	–
PO > PP	9.2	99%
PO > POP	10.4	99.4%
BO > PO	4.8	91%
BO > P	12.8	99.8%
BO > NP	5.2	97.8%
NP > P	4.6	90%
RP > PO	13.4	99.8%
C ≈ GOP	1.7	–
RP > C	7.9	98%
RP > GOP	13.0	99.8%
RP > BO	3.4	85%

Abbreviations: RP = radial pyroxene; C = cryptocrystalline; GOP = granular olivine-pyroxene; BO = barred olivine; PO = porphyritic olivine; PP = porphyritic pyroxene; POP = porphyritic olivine-pyroxene; $\chi^2 = (O - E)^2/E$ where O = observed value and E = expected value; P = porphyritic (PO + PP + POP), NP = nonporphyritic (RP + C + GOP).
*In each case, the χ^2 value is with two degrees of freedom.

chondrules (the largest porphyritic chondrules) and BO chondrules (Table 6). The other nonporphyritic chondrules (C, GOP) are not significantly different in size from each other and both varieties are significantly smaller than RP chondrules.

Chondrule Axial Ratios–The mean axial ratio (**b/a**) of LL3 chondrules is 0.82 ± 0.12 (Table 2). This value is similar to that determined previously (0.79) for six large separated Semarkona chondrules (Table 4 of Gooding, 1979), suggesting that axial ratio is largely independent of chondrule size. Bishunpur chondrules (**b/a** = 0.75 ± 0.15) have the lowest mean axial ratio, but this value is not significantly lower than those of the chondrules in the other LL3 chondrites: Semarkona, **b/a** = 0.81 ± 0.13; Krymka, 0.80 ± 0.12; Piancaldoli, 0.82 ± 0.12; LEW 88175, 0.85 ± 0.12.

Chondrule Fragments

Fragment Sizes in LL3 Chondrites–Figure 1b shows that the chondrule fragments in the five LL3 chondrites have a log-normal size-frequency distribution with a peak at 1.0–1.5 ϕ units (354–500 μm). The average apparent cross-section of the 1322 chondrule fragments (including isolated mafic silicate grains) >88 μm in apparent size in the five LL3 chondrites is 1.60 ± 0.84 ϕ units (330 μm) (Table 2) with a standard deviation of the sampling distribution ($\sigma/\sqrt{n}$) of 7 μm. As with the

TABLE 7. Apparent sizes and axial ratios of different fragment types in LL3 chondrites.

Fragment type	Number of frags	Size range	Mean cross-section	St. dev. (ϕ)	Mean axial ratio (**b/a**)	St. dev.
RP	19	1.83 to –1.88 ϕ (280 to 1840 μm)	0.62 ϕ (650 μm)	0.74	0.52	0.24
C	26	3.27 to –0.44 ϕ (100 to 1350 μm)	1.32 ϕ (400 μm)	0.83	0.64	0.21
GOP	50	2.63 to 0.03 ϕ (160 to 980 μm)	1.07 ϕ (480 μm)	0.70	0.37	0.26
BO	34	2.58 to –0.75 ϕ (170 to 1680 μm)	0.94 ϕ (520 μm)	0.72	0.72	0.16
PO	305	3.35 to –1.63 ϕ (98 to 3090 μm)	1.59 ϕ (330 μm)	0.84	0.66	0.17
PP	234	3.35 to –0.30 ϕ (98 to 1230 μm)	1.64 ϕ (320 μm)	0.77	0.66	0.17
POP	467	3.45 to –0.48 ϕ (92 to 1400 μm)	1.42 ϕ (370 μm)	0.76	0.66	0.15
Olivine grains*	118	3.50 to –0.42 ϕ (89 to 1340 μm)	2.30 ϕ (200 μm)	0.71	0.68	0.16
Pyroxene grains*	69	3.45 to 0.48 ϕ (92 to 720 μm)	0.87 ϕ (550 μm)	1.56	0.17	0.51
All fragments	1322	3.50 to –1.63 ϕ (89 to 3090 μm)	1.60 ϕ (330 μm)	0.84	0.66	0.16

Abbreviations: frags = chondrule fragments; st. dev. = standard deviation; RP = radial pyroxene; C = cryptocrystalline; GOP = granular olivine–pyroxene; BO = barred olivine; PO = porphyritic olivine; PP = porphyritic pyroxene; POP = porphyritic olivine–pyroxene.
*Olivine and pyroxene grains are isolated grains and grain fragments that were derived from phenocrysts within porphyritic chondrules.

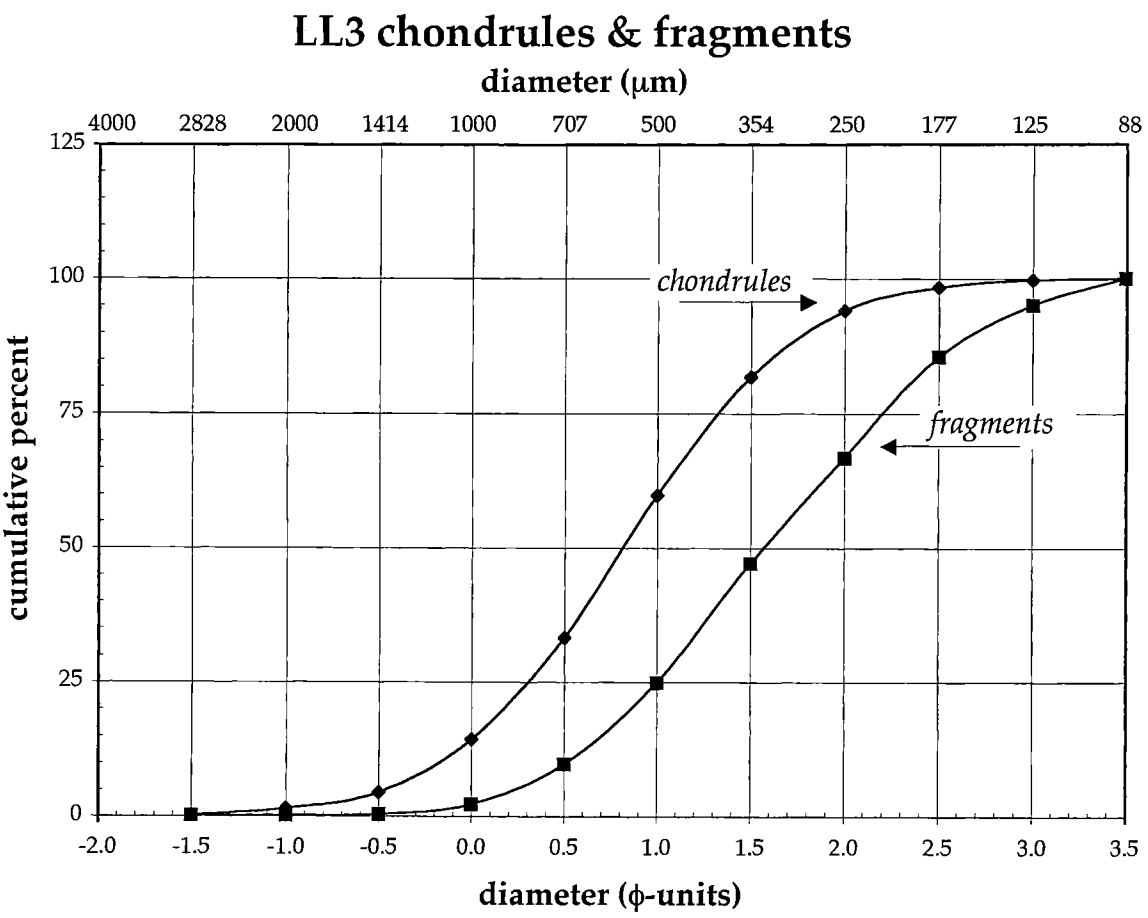

FIG. 4. Cumulative size-frequency diagram for chondrules and fragments in the five LL3 chondrites. Particle apparent sizes are given in both micrometers and ϕ units. The displacement of the fragment curve to the right of the chondrule curve indicates that fragments are much smaller than chondrules.

chondrule data, the mean fragment size was determined in ϕ units and then converted into micrometers.

The cumulative size-frequency diagram (Fig. 4) indicates that the fragment curve is displaced toward smaller sizes. The greatest differences between the curves occur at 1.0 and 1.5 ϕ units (500 and 354 μm): 60% of the chondrules but only 25% of the fragments are coarser than 1.0 ϕ; 82% of the chondrules but only 47% of the fragments are coarser than 1.5 ϕ.

Among the LL3 chondrites, Piancaldoli has the largest mean apparent cross-section of chondrule fragments (1.26 ϕ units; 420 μm) and Bishunpur the smallest (1.95 ϕ units; 260 μm) (Table 2; Fig. 5a,b).

Table 3 shows that the range in mean chondrule-fragment sizes among the six thin sections of Semarkona is 240 μm: USNM 1805-3 (0.88 ϕ units; 620 μm); USNM 1805-5 (1.63 ϕ units; 380 μm); UNM 312 (1.65 ϕ units; 380 μm); LC 229 (1.35 ϕ units; 450 μm); AMNH 4128-2 (0.98 ϕ units; 560 μm); and AMNH 4128-4 (1.53 ϕ units; 410 μm). This range is greater than that of the mean chondrule-fragment sizes in the five different LL3 chondrites (160 μm).

Proportions of Different Fragment Textural Types–The number percentages of textural types among the 1322 chondrule fragments in the five LL3 chondrites (Table 7) are: 35% POP, 18% PP, 23% PO, 3% BO, 1% RP, 2% C, 4% GOP, 9% isolated olivine grains and 5% isolated pyroxene grains. The proportions of chondrule fragments differ somewhat from those of intact chondrules (*i.e.*, 47% POP, 21% PP, 16% PO, 6% BO, 3% RP, 4% C and 3% GOP; Table 5). The fragment/intact-chondrule number ratios for the different textural types are: POP, 1.4; PP, 1.6; PO, 2.6; BO, 0.8; RP, 1.1; C, 0.8; and GOP, 2.2. If we include the isolated olivine and pyroxene grains among the porphyritic fragments, then the porphyritic fragment/intact-chondrule number ratio becomes 2.0, far higher than that of objects (BO + RP + C) with droplet textures (0.9).

The proportions of different fragment textural types differ at different size intervals (Table 8) (*i.e.*, different textural types of fragments have different mean diameters). For example, among the 129 largest fragments (those $\leq$0.5 ϕ units or $\geq$707 μm in average size), there are 6% BO, 2% C, 2% GOP, 25% PO, 45% POP, 11% PP, 7% RP, 2% isolated olivine grains, and

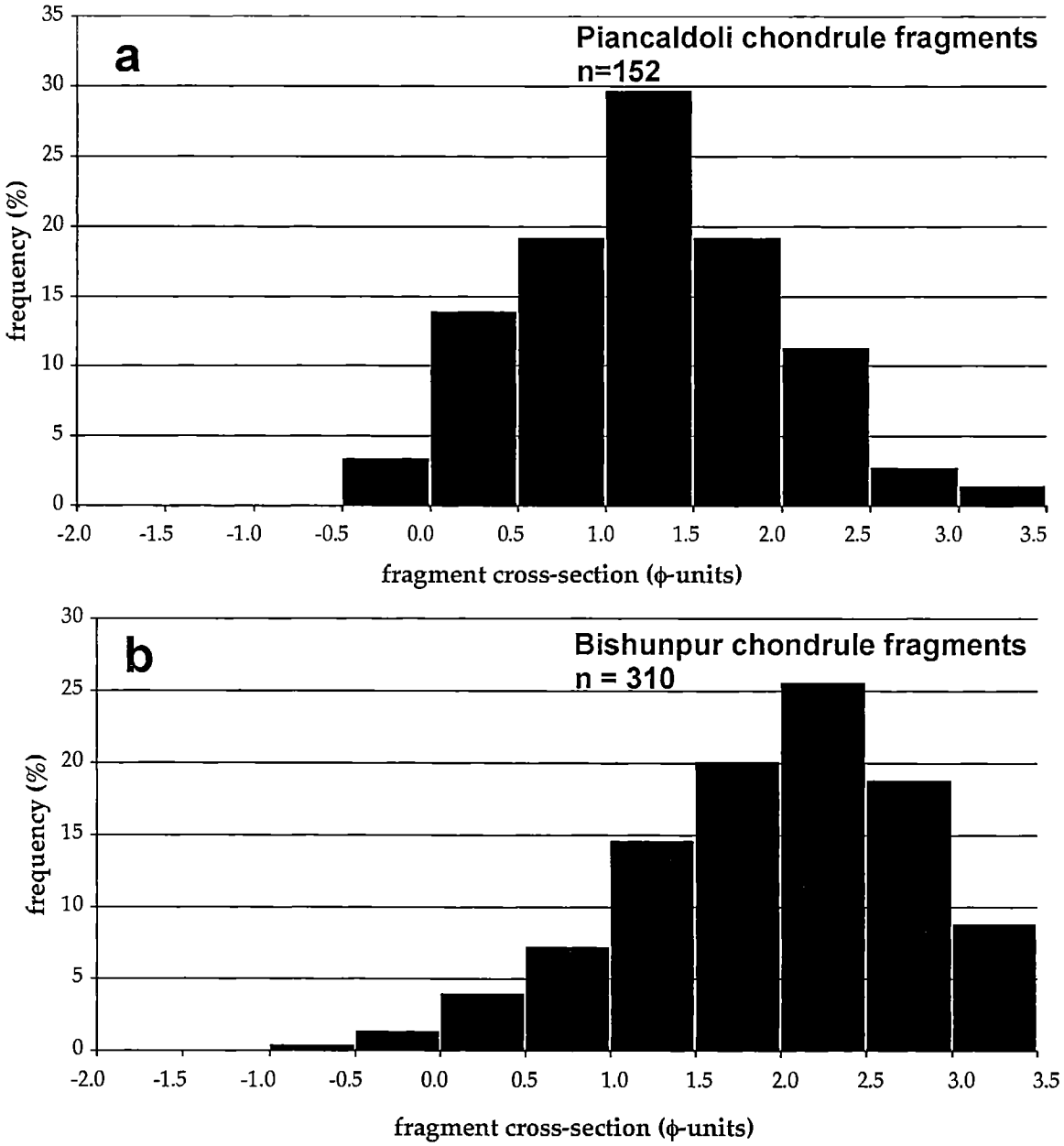

FIG. 5. Size-frequency distributions of chondrule fragments in two LL3 chondrites. (a) The 152 chondrule fragments measured in thin section in Piancaldoli. The mean apparent diameter of the fragments is 1.26 ϕ units (420 μm). (b) The 310 chondrule fragments measured in thin section in Bishunpur. The mean apparent diameter of the fragments is 1.95 ϕ units (260 μm), appreciably smaller than the fragments in Piancaldoli. This is clearly shown in the difference in the distribution peaks (1.0–1.5 *vs.* 2.0–2.5 ϕ units for Piancaldoli and Bishunpur, respectively). The abrupt cut-off on the right side of the Bishunpur fragment distribution indicates that a significant number of fragments smaller than 3.5 ϕ units were not counted in this study.

<1% isolated pyroxene grains. In contrast, among the 192 smallest fragments (those 2.5–3.5 ϕ units or 88–177 μm in average size), there are <1% BO, 2% C, 1% GOP, 26% PO, 17% POP, 13% PP, 0% RP, 26% isolated olivine grains, and 15% isolated pyroxene grains. The major differences are in RP fragments (7% among large objects *vs.* 0% among small objects), POP fragments (45% *vs.* 17%), isolated olivine grains (2% *vs.* 26%) and isolated pyroxene grains (<1% *vs.* 15%).

Size-frequency Distributions of Different Textural Types of Fragments–Some textural types of chondrule fragments appear larger, on average, than other types (Table 7). A series of Kolmogorov–Smirnov two-sample one-tailed statistical tests was performed to test the hypothesis that one

TABLE 8. Proportions of chondrule fragment types in different apparent size intervals for LL3 chondrites.

Size interval		Percentage of all chondrule fragments									Total no. of chondrule fragments
Cross-section (μm)	Cross-section (ϕ units)	RP	C	GOP	BO	PO	PP	POP	Olivine grains*	Pyroxene grains*	
2828 to 4000	−2.0 to −1.5	–	–	–	–	100.0	–	–	–	–	1
2000 to 2828	−1.5 to −1.0	–	–	–	–	–	–	–	–	–	0
1414 to 2000	−1.0 to −0.5	66.7	–	–	33.3	–	–	–	–	–	3
1000 to 1414	−0.5 to 0.0	4.0	4.0	–	4.0	24.0	16.0	44.0	4.0	–	25
707 to 1000	0.0 to 0.5	6.0	2.0	2.0	6.0	25.0	10.0	47.0	1.0	1.0	100
500 to 707	0.5 to 1.0	2.0	3.5	5.0	5.5	21.6	17.6	38.2	1.5	5.0	199
354 to 500	1.0 to 1.5	1.0	1.7	2.4	1.7	22.4	19.4	43.6	4.4	3.4	294
250 to 354	1.5 to 2.0	1.1	2.7	6.5	3.1	21.8	16.5	37.2	8.4	2.7	261
177 to 250	2.0 to 2.5	–	0.4	4.9	0.4	23.5	24.3	30.3	11.3	4.9	247
125 to 177	2.5 to 3.0	–	1.6	1.6	0.8	31.7	13.5	17.4	22.2	11.1	126
88 to 125	3.0 to 3.5	–	1.5	–	–	13.6	12.1	16.7	33.3	22.7	66

Abbreviations: RP = radial pyroxene; C = cryptocrystalline; GOP = granular olivine-pyroxene; BO = barred olivine; PO = porphyritic olivine; PP = porphyritic pyroxene; POP = porphyritic olivine–pyroxene.
*Olivine and pyroxene grains are isolated grains and grain fragments derived from phenocrysts within porphyritic chondrules.

textural type of fragment is significantly larger than another.

As shown in Table 9, although the BO fragments (Fig. 6a) are not significantly larger than the RP fragments (Fig. 6b), both fragment types are significantly larger than the PO fragments. Smallest of all are the isolated olivine and pyroxene grains (Fig. 6c; Table 9).

Axial Ratios of Fragments–The mean axial ratio (**b/a**) of chondrule fragments in LL3 chondrules is 0.66 ± 0.16 (Table 2), much lower than that of intact chondrules (0.82 ± 0.12).

Fragment/Intact-Chondrule Number Ratios in Different LL3 Chondrites

The five LL3 chondrites studied here have fragment/chondrule number ratios exceeding unity: Semarkona, 1.3; Bishunpur, 3.6; Krymka, 2.9; Piancaldoli, 1.7; and LEW 88175, 1.6. Because a single disrupted chondrule can produce numerous fragments, it is difficult to determine from the fragment/chondrule number ratio the percentage of chondrules that were shattered.

TABLE 9. Statistical significance of differences among textural types of chondrule fragments.

Fragment sets	χ^{2*}	Confidence level
BO ≈ RP	2.8	–
BO > PO	12.0	99.8%
RP > PO	13.7	99.9%
PO > ol	32.8	99.999%
PO > pyx	15.2	99.99%

Abbreviations: $\chi^2 = (O - E)^2/E$ where O = observed value and E = expected value; ol = isolated olivine grains; pyx = isolated pyroxene grains; BO = barred olivine; PO = porphyritic olivine; RP = radial pyroxene.
*In each case, the χ^2 value is with two degrees of freedom.

DISCUSSION

Sites of Chondrule Fragmentation

Chondrules could have been fragmented on the parent asteroid or in the solar nebula prior to accretion. It is clear that both processes occurred: (1) Grossman *et al.* (2000) demonstrated that "bleached" RP and C chondrules experienced parent-body aqueous alteration. The light-colored bleached zones are porous, depleted relative to unbleached regions in those elements likely to be contained in chondrule glass (*i.e.*, Na, K, Al, Sr, Si), and enriched in water, halogens, Fe, Ni and possibly Rb; the zones also contain phyllosilicates and pentlandite (Grossman *et al.*, 2000). Chondrule fragments that are bleached on rounded surfaces but not on a fractured surface (*e.g.*, Fig. 4c of Grossman *et al.*, 2000) were fragmented on the parent body (after an episode of aqueous alteration). (2) Rubin (1984) showed that coarse-grained (igneous) rims around chondrules were formed in the solar nebula by partly melting preexisting fine-grained dusty rims. Chondrule fragments that are completely surrounded by coarse-grained rims (*e.g.*, Fig. 1b of Rubin, 1984) must have been fragmented in the nebula (prior to acquisition by the chondrule of a dusty rim or entrainment of the chondrule in a fine-grained, porous dustball). Similarly, chondrule fragments within independent enveloping compound

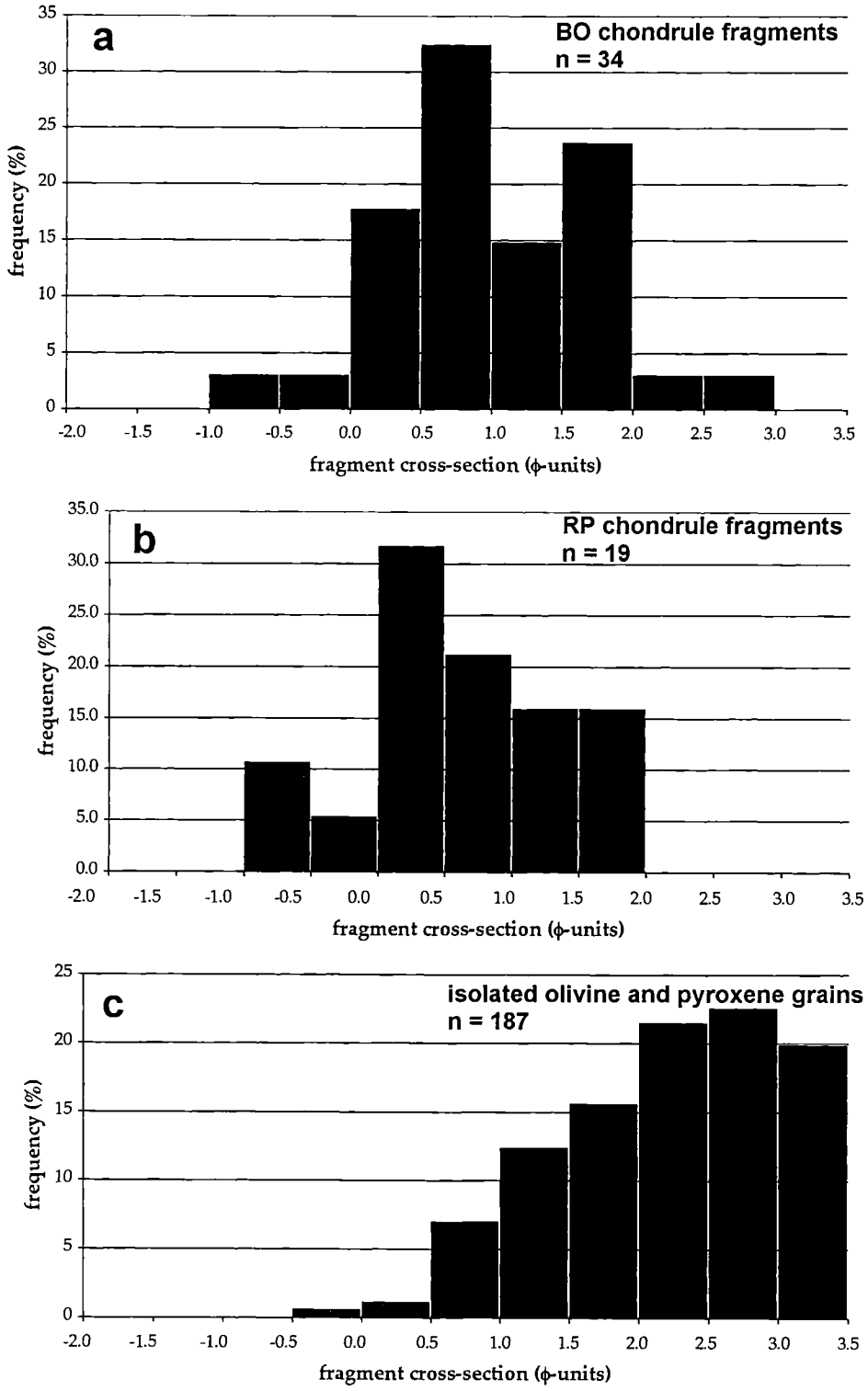

FIG. 6. Size-frequency distribution of specific textural types of chondrule fragments measured in thin section in five LL3 chondrites. (a) The 34 BO chondrule fragments peak at 0.5–1.0 ϕ units. (b) The 19 RP chondrule fragments peak at 0.0 to 0.5 ϕ units, but have a broad high ϕ value tail extending toward small sizes. The sizes of the RP fragments are not significantly different than those of BO fragments. (c) The 187 isolated olivine and pyroxene grains and grain fragments peak at 2.0–3.5 ϕ units and have a broad low ϕ value tail extending toward larger sizes. These objects are smaller than the other chondrule fragments. The abrupt cut-off on the right side of the distribution of isolated olivine and pyroxene grains indicates that a very large number of grains smaller than 3.5 ϕ units was not counted in this study.

chondrules (*e.g.*, Fig. 29 of Tschermak, 1885/1964; Fig. 3a,b of Wasson *et al.*, 1995) were broken in the nebula prior to a second chondrule-heating event.

There are reasons to conclude that most chondrules were fragmented on the parent body. Many chondrites are extensively shocked (*e.g.*, Stöffler *et al.*, 1991) or brecciated (*e.g.*, Rubin *et al.*, 1983), processes that can lead to chondrule fragmentation. For example, Vigarano (CV3) is a regolith breccia containing chondritic clasts as well as clastic matrix regions consisting of crushed chondrule and calcium-aluminum-rich inclusion (CAI) fragments and numerous isolated olivine and pyroxene grains (Rubin, 1984).

Individual chondrites vary significantly in the amount of parent-body processing (including brecciation and crushing) that they experienced. Among LL3 chondrites, there are numerous examples of meteorites exhibiting shock effects or containing clasts incorporated during parent-body brecciation events (Table 10). Thus, the significant differences among LL3 chondrites in their fragment/intact-chondrule number ratios are more likely to have resulted from parent-body brecciation than stochastic nebular processes.

Bishunpur and Krymka have the most extreme characteristics indicative of chondrule fragmentation. They have the highest fragment/intact-chondrule number ratios (3.6 and 2.9 in Bishunpur and Krymka, respectively, *vs.* 1.3–1.7 in Semarkona, Piancaldoli and LEW 88175) and the smallest mean fragment sizes (260 and 290 μm *vs.* 350–420 μm). The high fragment/chondrule number ratios and small fragment sizes in Bishunpur and Krymka appear to have resulted from shattering and crushing of previously intact chondrules. The paucity of large chondrules in Krymka (Fig. 2b) may have resulted from preferential impact fragmentation of large components.

Bishunpur has the least circular chondrules (*i.e.*, intact chondrules with the lowest mean axial ratio, that is, 0.75). We speculate that these low axial ratios may have resulted from shock deformation of chondrules (*e.g.*, Sneyd *et al.*, 1988) by processes analogous to those that caused alignment of chondrules and inclusions in CV3 Leoville (cf., Cain *et al.*, 1986). It seems likely that, by chance, Bishunpur and Krymka experienced more severe crushing than the other LL3 chondrites in the present study.

Because the shock stages of the LL3 chondrites in this study are low (all S1–S2 except for Krymka, S3; Table 1), the impacts that caused chondrule fragmentation must mainly have been of low energy.

The chondrule size-frequency distribution is log-normal and peaks at 0.5–1.0 ϕ units (Fig. 1a), whereas the fragment distribution is skewed toward smaller sizes (*i.e.*, there is a dearth of fragments coarser than 1.0 ϕ units (Fig. 1b)). This accounts for the large difference between the chondrule and fragment cumulative size-frequency curves at 1.0 ϕ (Fig. 4). Fragments are derived from shattered chondrules and are expected to peak at size ranges smaller than the chondrule peak.

Although the chondrule curve levels off at high ϕ values (*i.e.*, at very small sizes), the fragment curve does not. This indicates that many fragments smaller than the cut-off at 3.5 ϕ were excluded from the present study.

Fragmentation Differences Among Textural Types

The low abundance of fragments with BO, RP and C (*i.e.*, droplet) textures relative to fragments with porphyritic textures implies that droplet chondrules are less friable than porphyritic chondrules. If this is indeed the case, there should be a greater

TABLE 10. LL3 chondrites that have undergone significant parent-body processing.

Chondrite	Type	Clasts or shock effects	References
Acfer 160	LL3-6	Genomict breccia	1
Adzhi-Bogdo	LL3-6	Impact-melt-rock clasts, metamorphosed clasts, alkali-granitoid clasts	2
Allan Hills A76004	LL3.3	Shock-melted metal-sulfide intergrowths	3
Allan Hills A77278	LL3.7	Dark clast, possibly a carbonaceous chondrite	4
Allan Hills A79003	LL3.4	Shock-melted metal-sulfide intergrowths	3
Bhola	LL3-6	Impact-melt-rock clasts; shock-darkened clasts and metamorphosed clasts	1,5
Dar al Gani 022	LL3-6	Genomict breccia	1
Great Sand Sea 008	LL3-6	Genomict breccia	1
Krymka	LL3.1	Olivine-microchondrule-bearing clast	6
Ngawi	LL3.6	Regolith breccia with solar wind gases, impact-melt-rock clasts, metamorphosed clasts	7,8,9
Parnallee	LL3.7	Impact-melt-rock clasts	7,10
Piancaldoli	LL3.4	LL4 clast; chondritic clasts with different amounts of matrix	9,11
Quinyambie	LL3.4	LL3.0 clast; matrix-rich clast	12
Ragland	LL3.4	Clast with abundant silicate fragments derived from crushed chondrules	13
Richfield	LL3.7	Genomict breccia with LL5 clasts and impact-melt-rock clasts	14
Wells	LL3.3	Fragmental breccia with dark inclusions	15

References: 1 = Grady (2000); 2 = Bischoff *et al.* (1993); 3 = Scott *et al.* (1982); 4 = Marvin and Mason (1980); 5 = Fodor and Keil (1978); 6 = Rubin (1989b); 7 = Scott and Taylor (1982); 8 = Schultz and Kruse (1989); 9 = A. E. Rubin, unpubl. data; 10 = Binns (1967); 11 = Rubin *et al.* (1982); 12 = E. R. D. Scott, pers. comm., 2002; 13 = Recca *et al.* (1986); 14 = Rubin *et al.* (1996); 15 = Weisberg *et al.* (1998).

proportion of droplet-textured objects among intact chondrules than among fragments. Table 11 lists the numbers of droplet-textured objects (BO + RP + C) and porphyritic-textured objects (PO + PP + POP) among intact chondrules and chondrule fragments. We can erect a null hypothesis, H_0, that there is no significant difference between these textural types of chondrules and fragments. A χ^2 test yields a value of 41.4 with 5 degrees of freedom indicating that $\alpha < 0.0001$. We thus reject H_0 at the 99.99% confidence level and conclude that intact chondrules and chondrule fragments have different proportions of objects with droplet and porphyritic textures. Another way to examine these data is to infer the volumetric abundances of each chondrule and fragment textural type relative to that of all chondrules and fragments in the set (Table 11). We find that the (BO + RP + C)/(PO + PP + POP) chondrule ratio is 0.24 and the (BO + RP + C)/(PO + PP + POP) fragment ratio is 0.18. The lower ratio among the fragments demonstrates that the droplet chondrules are more likely to remain intact (and, hence, are less friable) than porphyritic chondrules.

It seems plausible that the larger mean size of intact droplet chondrules relative to intact porphyritic (PO, PP, POP) chondrules (0.51 ϕ or 700 μm *vs.* 0.84 ϕ or 560 μm) (Table 5) is not a relic of chondrule formation, but results from the preferential disruption of porphyritic chondrules during low-energy impacts into OC parent asteroids. The relative paucity of porphyritic chondrules among the set of large chondrules compared to the set of small chondrules (57% *vs.* 81%) suggests that large porphyritic chondrules were preferentially disrupted. (This is consistent with results of Rubin and Pernicka (1989) who found that large porphyritic chondrules crumble easily during mechanical separation of chondrules from ordinary chondrites; the 19 surviving separated chondrules in their study of H3.4 Sharps are 37% porphyritic and 63% droplet chondrules with RP and C textures.) The large numbers of grain boundaries in porphyritic chondrules may be responsible for their apparent friability. BO and RP chondrules, which tend to break only along surfaces parallel to the olivine or pyroxene bars, seem to be more resistant to breakage than porphyritic chondrules.

McSween (1977) concluded that isolated olivine and pyroxene grains in carbonaceous chondrites were derived from phenocrysts liberated from disrupted porphyritic chondrules. This view is consistent with the inferred friability of porphyritic chondrules in LL3 chondrites. Furthermore, the average sizes of the isolated olivine (200 μm) and pyroxene (550 μm) grains in this study are similar to those of many coarse phenocrysts in high-FeO porphyritic chondrules in ordinary chondrites (*e.g.*, Scott and Taylor, 1983).

Condensation in the solar nebula is unlikely to produce grains appreciably coarser than 1 μm (*e.g.*, Blum and Münch, 1993); thus, the much coarser (89–1340 μm) isolated silicate grains in the LL3 chondrites counted here are probably all chondrule fragments.

There is additional evidence from other chondrite groups that isolated mafic silicate grains are derived from chondrules: (1) The distributions of CaO *vs.* mol% Fa in isolated olivine grains in CI chondrites (Fig. 5 of Leshin *et al.*, 1997) are very similar to those of chondrules in other chondrite groups (*e.g.*, Fig. 6 of Scott and Taylor, 1983). (2) The compositional distributions of isolated olivine and low-Ca pyroxene grains in CO3.0 Colony are identical to those of olivine and low-Ca

TABLE 11. Inferred proportions of chondrule and fragment textural types.

Textural type	Intact chondrules			Chondrule fragments		
	n	Mean radius (μm)	Percent of total area*	*n*	Mean dimension (μm)	Percent of total area†
RP	18	450	6.3	19	650	5.6
C	31	280	4.2	26	400	2.9
GOP	23	230	2.1	50	480	8.0
BO	40	375	9.7	34	520	6.4
PO	115	330	21.5	305	330	23.1
PP	151	265	18.2	234	320	16.6
POP	341	270	42.7	467	370	44.4
ol	–	–	–	118	200	3.3
pyx	–	–	–	69	550	14.5
Total	719	285	100.0	1322	330	100.0

Area of each chondrule = πr^2; area of each fragment = (mean dimension)^2.
The percent of total area is related to vol% in three dimensions.
*$((\pi r^2)n/(\text{total area of all chondrules})) \times 100$.
†$\{(\text{mean dimension})^2 \times n/(\text{total area of all fragments})\} \times 100$.
Abbreviations: *n* = number of objects; RP = radial pyroxene; C = cryptocrystalline; GOP = granular olivine-pyroxene; BO = barred olivine; PO = porphyritic olivine; PP = porphyritic pyroxene; POP = porphyritic olivine-pyroxene; ol = isolated olivine grains; pyx = isolated pyroxene grains.

pyroxene phenocrysts in Colony chondrules (Rubin *et al.*, 1985). (3) Isolated olivine grains in CO3 and CM2 chondrites contain small glass inclusions formed from trapped melt that are identical to those within olivine grains in porphyritic chondrules in the same meteorites (McSween, 1977).

SUMMARY

The mean apparent diameter of chondrules in five LL3 chondrites is 0.80 ϕ units or 570 μm. Chondrule fragments are much smaller than intact chondrules; fragments have a mean apparent cross-section of 1.60 ϕ units or 330 μm. The smallest fragments are isolated olivine and pyroxene grains; these are probably phenocrysts derived from shattered porphyritic chondrules. Most chondrule fragmentation probably occurred on the parent asteroid. Porphyritic chondrules (PO + PP + POP) are more readily broken than droplet chondrules (BO + RP + C). Differences in mean size among chondrule textural types may be due primarily to chondrule fragmentation on the parent asteroid, not to chondrule-formation processes in the solar nebula.

Acknowledgements–We thank J. T. Wasson for helpful discussions. We gratefully acknowledge useful reviews by I. S. Sanders and G. J. Taylor and the helpful comments of associate editor D. W. Mittlefehldt. One of us (V. E. N.) thanks R. L. Weiss and the Center for Academic and Research Excellence at UCLA for 3 months of support. This work was also supported in part by NASA grant NAG5-4766 (A. E. Rubin).

Editorial handling: D. W. Mittlefehldt

REFERENCES

BENOIT P. H., SYMES S. J. K. AND SEARS D. W. G. (1999) Chondrule size distributions: What does it mean? (abstract). *Lunar Planet. Sci.* **30**, #1053, Lunar and Planetary Institute, Houston, Texas, USA (CD-ROM).

BINNS R. A. (1967) An exceptionally large chondrule in the Parnallee meteorite. *Mineral. Mag.* **36**, 319–324.

BISCHOFF A., GEIGER T., PALME H., SPETTEL B., SCHERER P., SCHLÜTER J. AND LKHAMSUREN J. (1993) Mineralogy, chemistry, and noble gas contents of Adzhi-Bogdo—An LL3-6 chondritic breccia with L-chondritic and granitoidal clasts. *Meteoritics* **28**, 570–578.

BLUM J. AND MÜNCH M. (1993) Experimental investigations on aggregate-aggregate collisions in the early solar nebula. *Icarus* **106**, 151–167.

CAIN P. M., MCSWEEN H. Y. AND WOODWARD N. B. (1986) Structural deformation of the Leoville chondrite. *Earth Planet. Sci. Lett.* **77**, 165–175.

DODD R. T. (1976) Accretion of the ordinary chondrites. *Earth Planet. Sci. Lett.* **30**, 281–291.

EISENHOUR D. D. (1996) Determining chondrule size distributions from thin-section measurements. *Meteorit. Planet. Sci.* **31**, 243–248.

FODOR R. V. AND KEIL K. (1978) Catalog of lithic fragments in LL-group chondrites. *UNM Inst. Meteoritics, Sp. Pub.* **19**, 1–38.

GOODING J. L. (1979) Petrogenetic properties of chondrules in unequilibrated H-, L-, and LL-group chondritic meteorites. Ph.D. dissertation, Univ. New Mexico, Albuquerque, New Mexico, USA. 392 pp.

GOODING J. L. AND KEIL K. (1981) Relative abundances of chondrule primary textural types in ordinary chondrites and their bearing on conditions of chondrule formation. *Meteoritics* **16**, 17–43.

GRADY M. M. (2000) *Catalogue of Meteorites, Fifth Edition.* Cambridge University Press, Cambridge, U. K. 689 pp.

GROSSMAN J. N. AND WASSON J. T. (1982) Evidence for primitive nebular components in chondrules from the Chainpur chondrite. *Geochim. Cosmochim. Acta* **46**, 1081–1099.

GROSSMAN J. N. AND WASSON J. T. (1985) The origin and history of the metal and sulfide components of chondrules. *Geochim. Cosmochim. Acta* **49**, 925–939.

GROSSMAN J. N., RUBIN A. E., NAGAHARA H. AND KING E. A. (1988) Properties of chondrules. In *Meteorites and the Early Solar System* (eds. J. F. Kerridge and M. S. Matthews), pp. 619–659. Univ. Arizona Press, Tucson, Arizona, USA.

GROSSMAN J. N., ALEXANDER C. M. O'D., WANG J. AND BREARLEY A. J. (2000) Bleached chondrules: Evidence for widespread aqueous processes on the parent asteroids of ordinary chondrites. *Meteorit. Planet. Sci.* **35**, 467–486.

HUGHES D. W. (1978) A disaggregation and thin section analysis of size and mass distributions of the chondrules in the Bjurböle and Chainpur meteorites. *Earth Planet. Sci. Lett.* **38**, 391–400.

KING T. V. V. AND KING E. A. (1978) Grain size and petrography of C2 and C3 carbonaceous chondrites. *Meteoritics* **13**, 47–72.

KING T. V. V. AND KING E. A. (1979) Size frequency distributions of fluid drop chondrules in ordinary chondrites. *Meteoritics* **14**, 91–96.

LESHIN L. A., RUBIN A. E. AND MCKEEGAN K. D. (1997) The oxygen isotopic composition of olivine and pyroxene from CI chondrites. *Geochim. Cosmochim. Acta* **61**, 835–845.

MARTIN P. M. AND MILLS A. A. (1976) Size and shape of chondrules in the Bjurböle and Chainpur meteorites. *Earth Planet. Sci. Lett.* **33**, 239–248.

MARTIN P. M. AND MILLS A. A. (1978) Size and shape of near-spherical Allegan chondrules. *Earth Planet. Sci. Lett.* **38**, 385–390.

MARVIN U. B. AND MASON B. (1980) Catalog of Antarctic meteorites, 1977–1978. *Smithson. Contrib. Earth Sci.* **23**, 1–50.

MCSWEEN H. Y. (1977) On the nature and origin of isolated olivine grains in carbonaceous chondrites. *Geochim. Cosmochim. Acta* **41**, 411–418.

NAGAHARA H. (1981) Petrology of chondrules in ALH-77015 (L3) chondrite. *Mem. Natl. Polar Res., Special Issue* **20**, 145–160.

RECCA S. I. *ET AL.* (1986) Ragland, an LL3.4 chondrite find from New Mexico. *Meteoritics* **21**, 217–229.

RUBIN A. E. (1984) Coarse-grained chondrule rims in type-3 chondrites. *Geochim. Cosmochim. Acta* **48**, 1779–1789.

RUBIN A. E. (1989a) Size-frequency distributions of chondrules in CO3 chondrites. *Meteoritics* **24**, 179–189.

RUBIN A. E. (1989b) An olivine-microchondrule-bearing clast in the Krymka meteorite. *Meteoritics* **24**, 191–192.

RUBIN A. E. (1990) Kamacite and olivine in ordinary chondrites: Intergroup and intragroup relationships. *Geochim. Cosmochim. Acta* **54**, 1217–1232.

RUBIN A. E. AND KEIL K. (1984) Size-distributions of chondrule types in the Inman and Allan Hills A77011 L3 chondrites. *Meteoritics* **19**, 135–143.

RUBIN A. E. AND PERNICKA E. (1989) Chondrules in the Sharps H3 chondrite: Evidence for intergroup compositional differences among ordinary chondrite chondrules. *Geochim. Cosmochim. Acta* **53**, 187–195.

RUBIN A. E., SCOTT E. R. D. AND KEIL K. (1982) Microchondrule-bearing clast in the Piancaldoli LL3 meteorite: A new kind of type 3 chondrite and its relevance to the history of chondrules. *Geochim. Cosmochim. Acta* **46**, 1763–1776.

RUBIN A. E., REHFELDT A., PETERSON E., KEIL K. AND JAROSEWICH E. (1983) Fragmental breccias and the collisional evolution of ordinary chondrite parent bodies. *Meteoritics* **18**, 179–196.

RUBIN A. E., JAMES J. A., KECK B. D., WEEKS K. S., SEARS D. W. G. AND JAROSEWICH E. (1985) The Colony meteorite and variations in CO3 chondrite properties. *Meteoritics* **20**, 175–196.

RUBIN A. E., BENOIT P., REED B., EUGSTER O. AND POLNAU E. (1996) The Richfield LL3 chondrite. *Meteorit. Planet. Sci.* **31**, 925–927.

SCHULTZ L. AND KRUSE H. (1989) Helium, neon, and argon in meteorites—A data compilation. *Meteoritics* **24**, 155–172.

SCOTT E. R. D. AND TAYLOR G. J. (1982) Primitive breccias among type 3 ordinary chondrites—Origin and relation to regolith breccias. In *Workshop on Lunar Breccias and Soils and Their Meteoritic Analogs* (eds. G. J. Taylor and L. L. Wilkening), pp. 130–134. LPI Tech. Rpt. **82-02**, Lunar and Planetary Institute, Houston, Texas, USA.

SCOTT E. R. D. AND TAYLOR G. J. (1983) Chondrules and other components in C, O, and E chondrites: Similarities in their properties and origins. *Proc. Lunar Planet. Sci. Conf.* **14th**, B275–B286.

SCOTT E. R. D., TAYLOR G. J. AND MAGGIORE P. (1982) A new LL3 chondrite, Allan Hills A79003, and observations on matrices in ordinary chondrites. *Meteoritics* **17**, 65–76.

SNEYD D. S., MCSWEEN H. Y., SUGIURA N., STRANGWAY D. W. AND NORD G. L. (1988) Origin of petrofabrics and magnetic anisotropy in ordinary chondrites. *Meteoritics* **23**, 139–149.

STÖFFLER D., KEIL K. AND SCOTT E. R. D. (1991) Shock metamorphism of ordinary chondrites. *Geochim. Cosmochim. Acta* **55**, 3845–3867.

TILL R. (1974) *Statistical Methods for the Earth Scientist: An Introduction*. Wiley, New York, New York, USA. 154 pp.

TSCHERMAK G. (1885/1964) Die mikroskopische Beschaffenheit der Meteoriten. *Smithson. Contrib. Astrophys.* **4**, 138–239.

WASSON J. T. AND WANG S. (1991) The histories of ordinary chondrite parent bodies: U,Th-He age distributions. *Meteoritics* **26**, 161–167.

WASSON J. T., KROT A. N., LEE M. S. AND RUBIN A. E. (1995) Compound chondrules. *Geochim. Cosmochim. Acta* **59**, 1847–1869.

WEISBERG M. K., PRINZ P., ZOLENSKY M. E., CLAYTON R. N. AND MAYEDA T. K. (1998) Petrologic and oxygen isotopic study of dark inclusions in the Wells LL3 ordinary chondrite (abstract). *Lunar Planet. Sci.* **29**, #1882, Lunar and Planetary Institute, Houston, Texas, USA (CD-ROM).